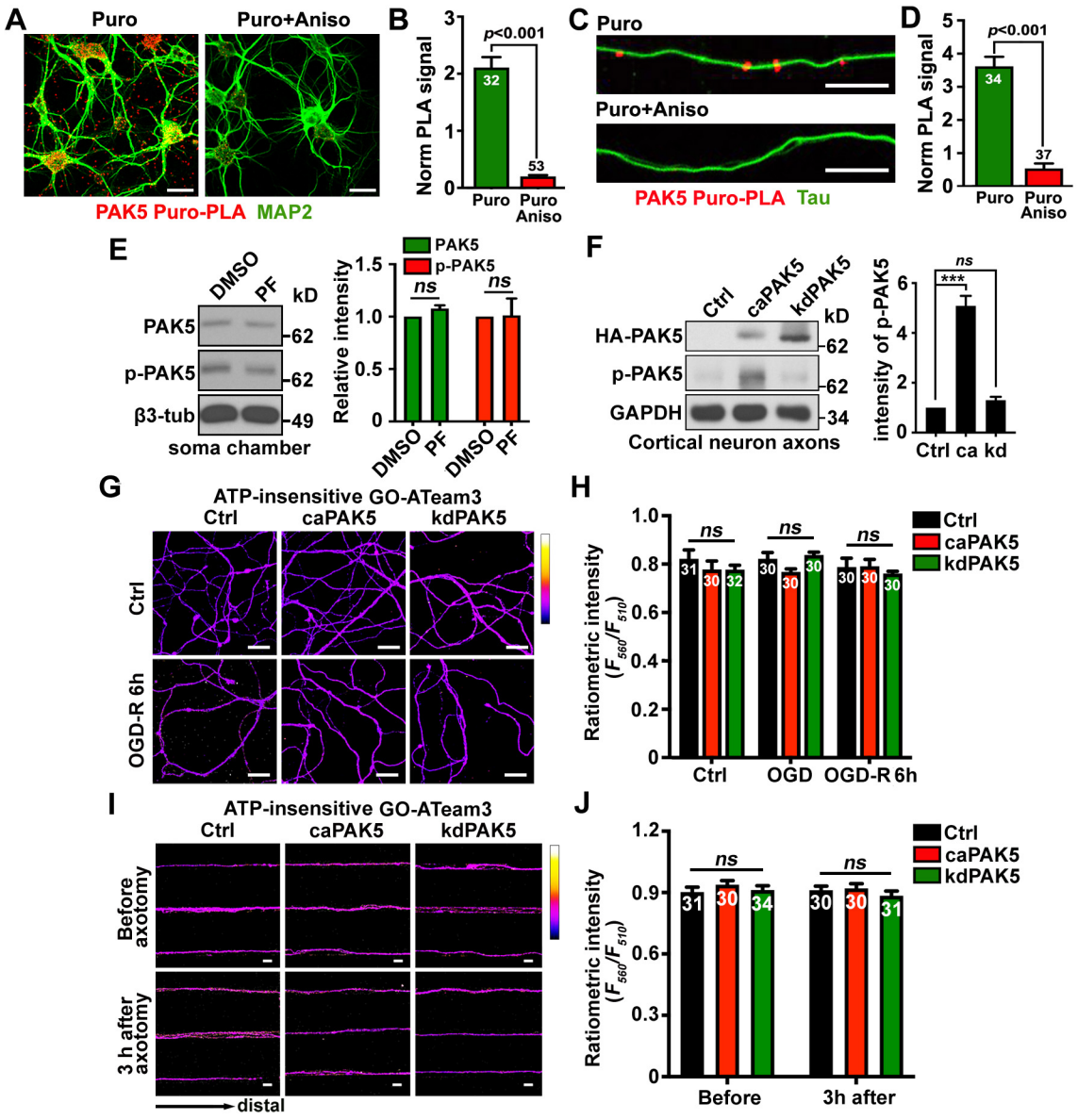

Figure S1. Validation of PAK5 Puro-PLA and ATP-insensitive probe GO-ATeam3. Related to Figures 1 and 2

(A-D) Representative Puro-PLA images (A, C) and analyses (B, D) showing newly synthesized PAK5 in neurons. Cortical neurons at DIV10 were incubated with 3 μM puromycin (Puro) for 15 min before fixation. For inhibiting protein synthesis, neurons were preincubated for 30 min with 40 μM anisomycin (Aniso). PAK5 Puro-PLA signals overlapped with MAP2-labeled soma-dendritic areas (A) or with Tau-labeled axons (C) and normalized to the MAP2 (B) or Tau signal area (D). Note that anisomycin abolishes PAK5 Puro-PLA signals in soma-dendritic area and axons, thus validating the Puro-PLA assay for labeling newly synthesized PAK5 in neurons.

(E) Soma-dendritic compartments display no significant PAK5 activation. Cortical neurons at DIV14 were treated with DMSO or PF-3758309 (1 μM) in the axon chamber for 3 hours, followed by lysate collection from soma-dendritic chambers and immunoblotting (5 μg). The intensity of PAK5 and p-PAK5 was quantified from three repeats (n = 3), calibrated with β3-tubulin levels, and normalized to the PAK5 or p-PAK5 expression in the DMSO group.

(F) Local expression of caPAK5 and kdPAK5 within axonal compartments. Cortical neurons in microfluidic devices were infected with lentiviruses encoding HA-tag (Ctrl), HA-tagged caPAK5 (ca) or kdPAK5 (kd) at DIV7. Axoplasmic lysates were collected from axon chambers at DIV14, followed by immunoblotting lysates (5 µg). The intensity of p-PAK5 was quantified from three repeats (n = 3), calibrated with GAPDH, and normalized to the control group. Note that expressing caPAK5, but not kdPAK5, activates PAK5 (p-PAK5) within axon compartments.
(G-J) Pseudo-color ratiometric images (G, I) and F_{560nm}/F_{510nm} ratiometric intensities (H, J) of ATP-insensitive GO-ATeam3 (R122K/R126K) after ischemic stress or axotomy. Cortical neurons in microfluidic devices were co-infected with lentiviruses expressing GO-ATeam3 and HA-tag control, HA-tagged caPAK5 or kdPAK5, followed by imaging axon chambers before or 6 hours after reperfusion following OGD treatment (G, H), or followed by imaging axonal bundles within the distal 150-µm microgroove region before or 3 hours after axotomy (I, J). Note that expressing GO-ATeam3 shows no significant change in the F_{560nm}/F_{510nm} ratiometric intensity after ischemic stress or axotomy.
Data were quantified from n = 30-53 images indicated in bar graphs in n > 3 microfluidic devices per condition from three independent experiments, expressed as mean ± SEM, and analyzed by Student's t test (B, D, E) or one-way ANONA with Dunnett's multiple comparisons test (F, H, J). Scale bars: 10 µm (C, G), 20 µm (A), and 25 µm (I).

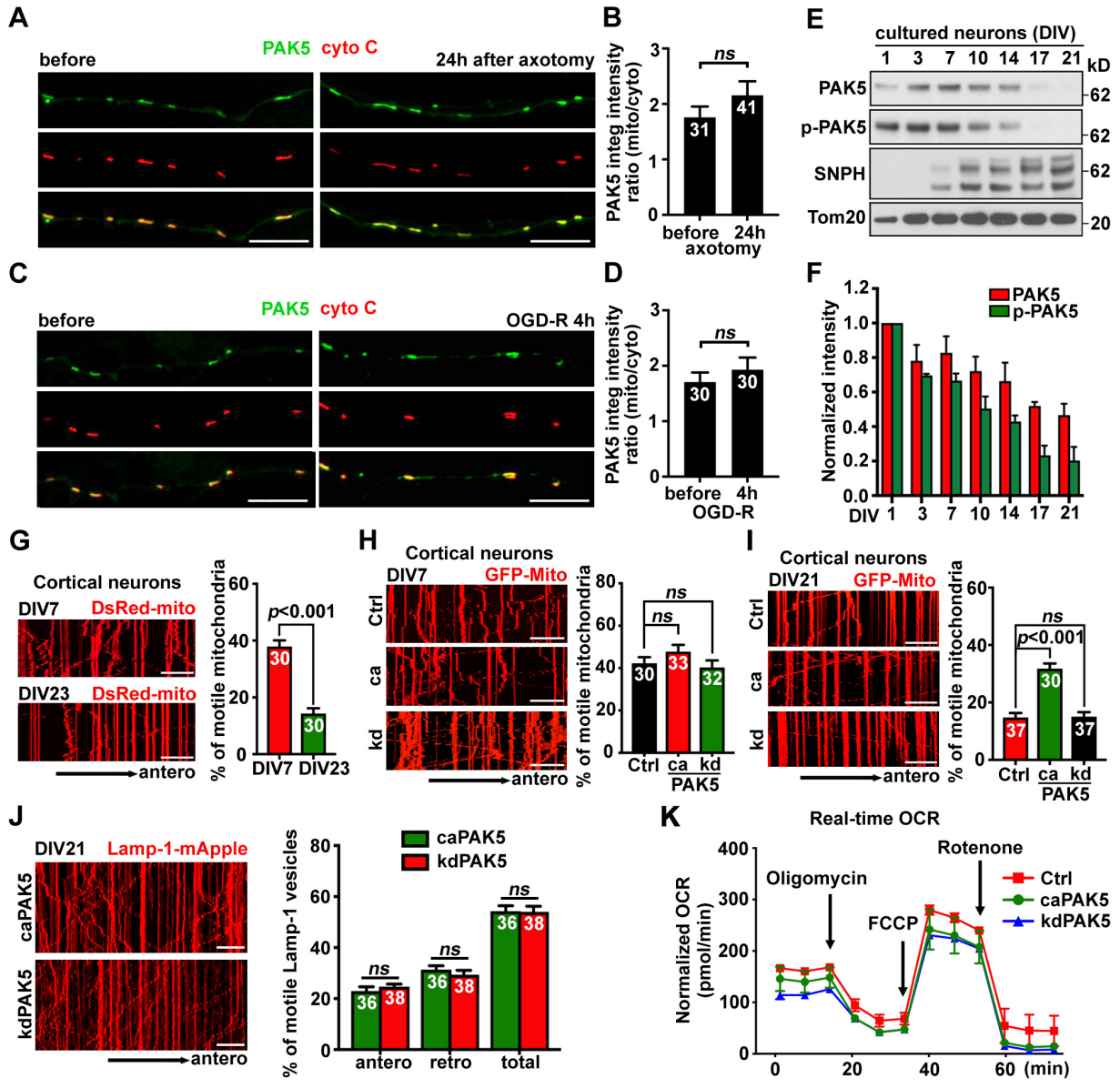

Figure S2. PAK5 activation enhances axonal mitochondrial transport. Related to Figure 3

(A-D) Images (A, C) and analyses (B, D) showing no significant change in axonal PAK5 distribution in mitochondria *vs* cytosol after axotomy or ischemic stress. Mature cortical neurons (DIV14) in microfluidic devices were fixed before or 24 hours after axotomy (A, B) or 4 hours after OGD-R (C, D), followed by co-immunostaining with PAK5 and Cyto c. The ratio of the integrated intensity of PAK5 between mitochondria and axonal cytosol was measured using ImageJ.

(E and F) Immunoblots (E) and analysis (F) showing progressive decline of total PAK5 expression and its activated form p-PAK5, and the opposing increases in SNPH expression with neuron maturation. Cortical neurons isolated from E18 mouse brains were cultured for 1, 3, 7, 10, 14, 17, and 21 days. Equal amounts (10 μg) of cell lysates were loaded and sequentially immunoblotted with indicated antibodies. The intensity of PAK5 or p-PAK5 bands was quantified from three repeats (n = 3), calibrated with TOM20 levels, and normalized to PAK5 or p-PAK5 at DIV1.

(G) Mature neuron-associated decline of axonal mitochondrial transport. Cortical neurons were transfected with DsRed-mito at DIV4 and imaged at DIV7 (young neurons), or transfected with

DsRed-mito at DIV10 and imaged at DIV23 (mature neurons). Time-lapse imaging was recorded for 90 frames with 5-sec intervals. In kymographs, vertical lines represent stationary mitochondria; oblique lines or curves to the right indicate anterograde transport; oblique lines or curves to the left indicate retrograde transport. Note that compared with young neurons (DIV7), axonal mitochondrial transport in mature neurons (DIV23) is significantly decreased.

(H and I) PAK5 activation fails to enhance axonal mitochondrial transport in young neurons at DIV7 (H) but reverses declined axonal mitochondrial transport in mature neurons at DIV21 (I). Cortical neurons at DIV1 or DIV15 were co-infected with lentiviruses encoding GFP-Mito and HA-tag control, HA-tagged caPAK5, or kdPAK5, followed by time-lapse imaging for 90 frames with 5-sec intervals at DIV7 or DIV21, respectively. Note that expressing caPAK5 ($P < 0.001$), but not kdPAK5, reverses declined axonal mitochondrial transport in mature neurons.

(J) PAK5 activation fails to affect endolysosome transport in mature cortical neurons at DIV21. Neurons at DIV15 were infected with lentiviruses encoding LAMP-1-mApple and HA-tagged caPAK5 or kdPAK5, followed by time-lapse imaging at DIV21 (90 frames with 2-sec intervals).

(K) Mitochondrial bioenergetics assessment with Seahorse XF analyzer showing no significant change in oxygen consumption rate (OCR) following expression of caPAK5 or kdPAK5 in neurons. Cortical neurons at DIV7-8 were infected with lentiviruses encoding caPAK5 or kdPAK5. Real-time baseline OCR was measured at DIV14 before and after sequential injection of ATP synthase inhibitor oligomycin, mitochondrial uncoupler FCCP, and mitochondrial complex I inhibitor rotenone into each cell well ($8x10^6$ cells) at the indicated time points (each point $n > 7$ wells).

Data were quantified from $n = 30$-41 axonal images (B, D), or $n = 30$-38 neurons (G-J) as indicated within bars from three independent experiments, expressed as mean ± SEM, and analyzed by one-way ANOVA with Dunnett's multiple comparisons test (H, I) or Student's *t* test (B, D, G, J). Scale bars, 10 μm.

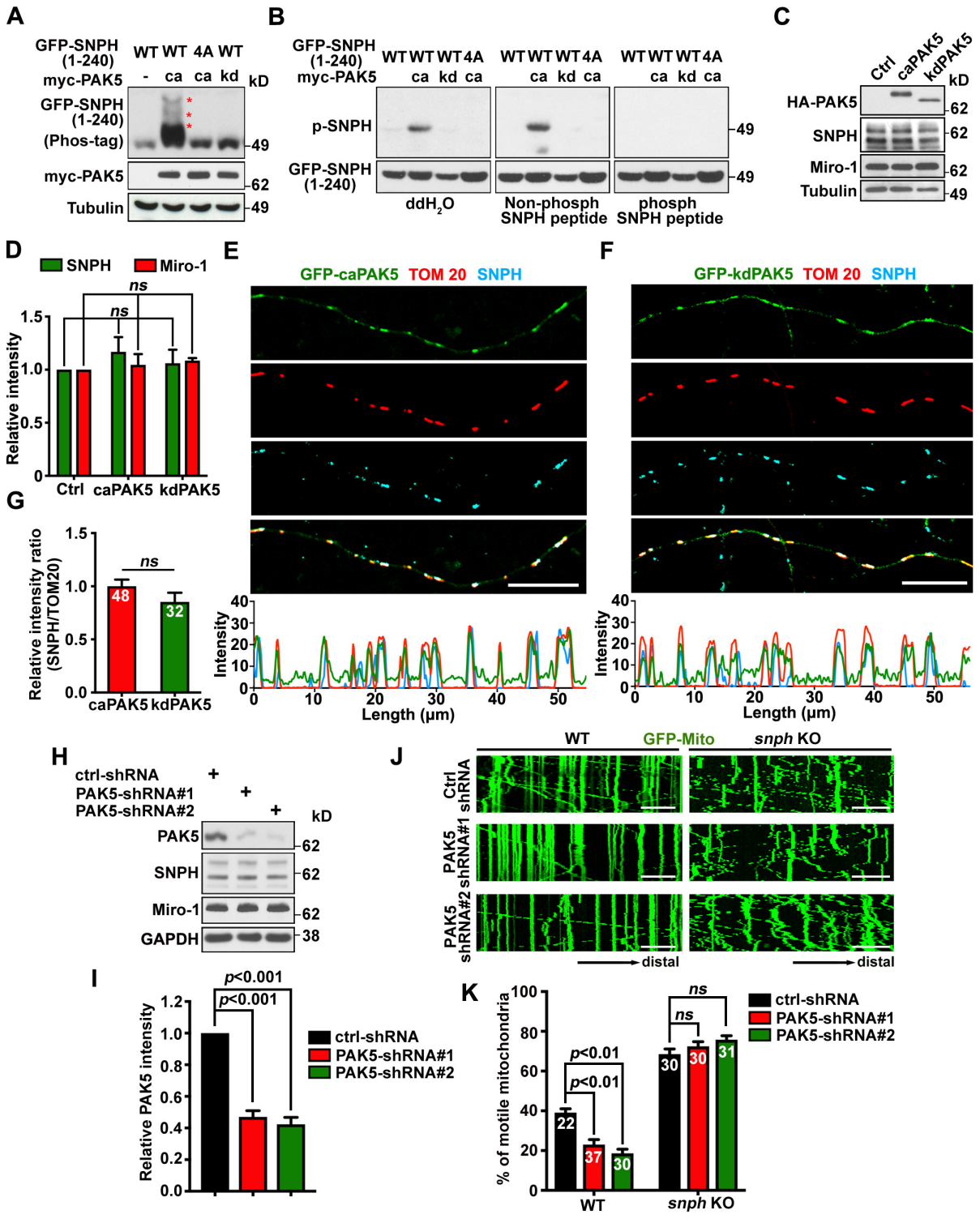

Figure S3. **PAK5-SNPH axis facilitates axonal mitochondrial transport. Related to Figure 4**
(A) Activating PAK5 mediates the phosphorylation of SNPH, but not the phospho-dead SNPH-4A mutant in which all four serine/threonine residues were replaced by alanine. HEK293T cells were co-transfected with the indicated vectors, and cell lysates (10 μg) were loaded into Phos-Tag SDS-PAGE gels and sequentially immunoblotted with the indicated antibodies. Asterisks mark the

phospho-shifted SNPH bands. Note that kdPAK5 failed to mediate SNPH phosphorylation.
(B) Specificity of the anti-phospho-SNPH antibody (anti-p-SNPH). The anti-p-SNPH antibody was preincubated with non-phospho- or phospho-SNPH peptide at a 5:1 ratio (peptide:antibody) for 1 hour at room temperature. Note that the phospho-SNPH peptide blocks the detection of p-SNPH.
(C and D) Immunoblots (C) and analysis (D) showing the expression of caPAK5 and kdPAK5 in cortical neurons. Neurons were infected with lentiviruses encoding HA-tag, HA-tagged caPAK5 or kdPAK5 at DIV7. After lysate collection at DIV14, 8-μg of lysates were loaded and sequentially immunoblotted with the indicated antibodies. The intensity of SNPH or Miro-1 bands was quantified from three repeats (n = 3), calibrated with tubulin levels, and normalized to the intensity of SNPH or Miro-1 bands in control neurons.
(E-G) Images (E and F) and analysis (G) showing that activating PAK5 does not impact SNPH expression on axonal mitochondria. Cortical neurons were transfected with GFP-caPAK5 or kdPAK5 at DIV7, followed by co-immunostaining with TOM20 and SNPH at DIV14. The distribution of GFP-tagged PAK5 (green), TOM20 (red), and SNPH (blue) along axons was analyzed using intensity profiles. Relative SNPH expression on individual axonal mitochondria was assessed by measuring the mean integrated intensity ratio of SNPH/TOM20. Note that both caPAK5 and kdPAK5 target to axonal mitochondria.
(H and I) Immunoblots (H) and quantitative analysis (I) showing knockdown efficiency of PAK5-shRNAs in cortical neurons. Neurons were infected with lentiviruses encoding control shRNA (ctrl-shRNA) or two different mouse PAK5-shRNAs at DIV2. Following harvesting at DIV10, cell lysates (10 μg) were sequentially immunoblotted with the indicated antibodies. The intensity of PAK5 bands was quantified from three repeats (n = 3), calibrated with GAPDH levels, and normalized to the PAK5 expression in ctrl-shRNA. Note that both PAK5-shRNAs effectively deplete PAK5 in cortical neurons without affecting expression of mitochondrial proteins Miro-1 and SNPH.
(J and K) Kymographs (J) and analysis (K) showing axonal mitochondrial transport in WT or *snph* KO neurons upon PAK5 depletion. Cortical neurons were co-infected with lentiviruses encoding GFP-Mito and PAK5-shRNAs at DIV3, followed by time-lapse imaging at DIV10 (90 frames with 5-sec intervals). Note that PAK5 depletion reduces mitochondrial transport in WT, but not in *snph* KO neurons, indicating a crucial role for PAK5 in turning off SNPH-mediated anchoring.
Data were quantified from the total number of neurons indicated within bars from three independent experiments, expressed as mean ± SEM, and analyzed by Student's t test (G) or one-way ANONA with Dunnett's multiple comparisons test (D, I, K). Scale bars, 10 μm.

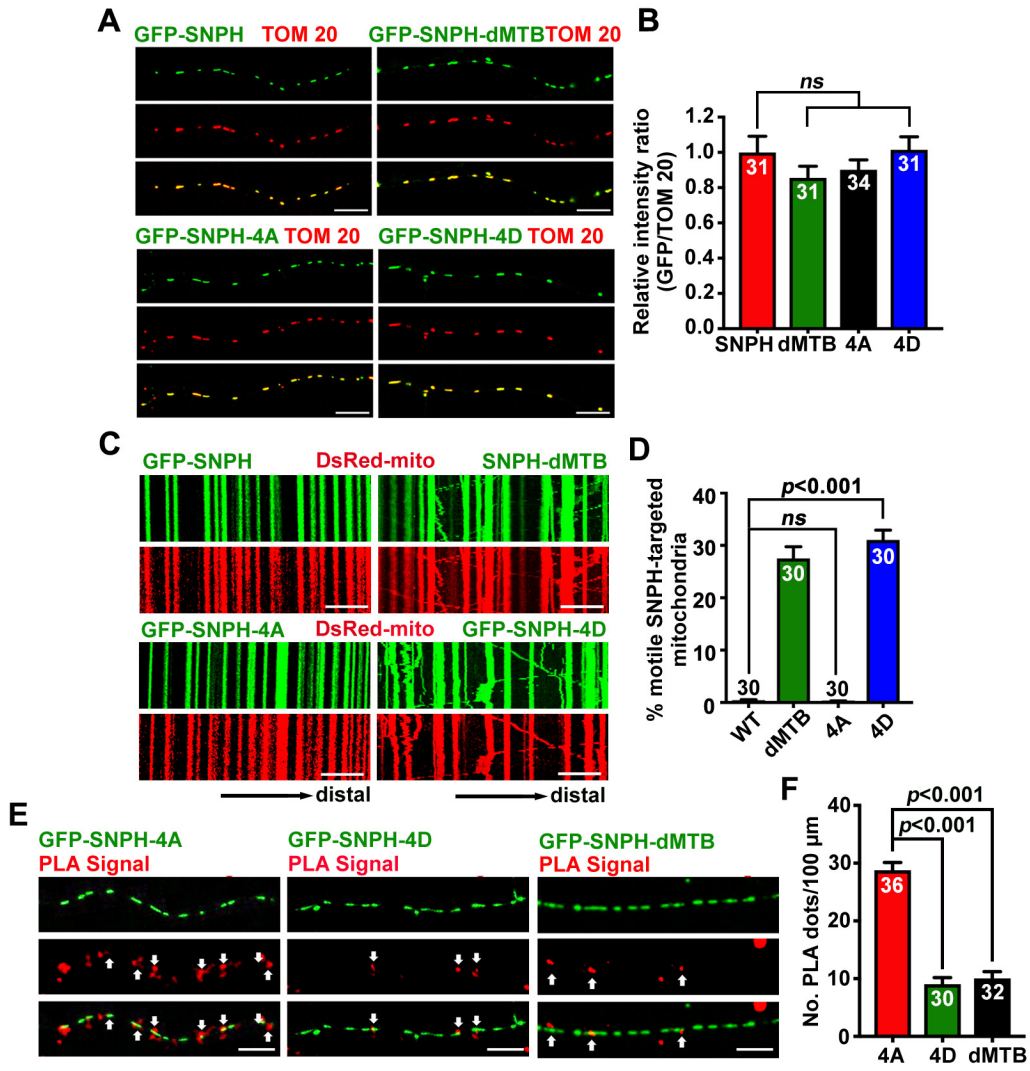

Figure S4. Clustered SNPH phosphorylation turns off its mitochondrial anchoring switch. Related to Figure 4

(A and B) Images (A) and analysis (B) showing a similar pattern of axonal mitochondria-targeting of WT SNPH and its three mutants. Cortical neurons were transfected with GFP-tagged SNPH, SNPH-dMTB, SNPH-4A, or SNPH-4D at DIV7, followed by immunostaining with TOM20 at DIV14. The relative levels of SNPH and its mutants on individual axonal mitochondria were assessed by the mean integrated intensity ratio of GFP/TOM20.

(C and D) Kymographs (C) and analysis (D) showing enhanced motility of axonal mitochondria following clustered phosphorylation of SNPH. Cortical neurons at DIV7 were co-transfected with DsRed-mito and GFP-SNPH, phospho-dead SNPH-4A, phospho-mimicking SNPH-4D, or anchoring loss-of-function mutant SNPH-dMTB, followed by time-lapse imaging at DIV10 (90 frames with 5-sec intervals).

(E and F) PLA images (E) and analysis (F) showing *in situ* MT-association of SNPH phosphorylation mutants along axons. SNPH-dMTB was used as a MT-binding loss-of-function mutant. Cortical neurons were transfected with GFP-tagged SNPH-4A, SNPH-4D, or SNPH-dMTB at DIV7, followed by PLA at DIV10. Arrows mark PLA signals that reflect *in situ* SNPH-MT association in axons. The number of PLA signals per 100-µm axon length was quantified. Note

that phospho-mimicking SNPH-4D, but not phospho-dead SNPH-4A, loses its MT-binding capacity.
Data were quantified from the total number of neurons indicated within bars from three independent experiments, expressed as mean ± SEM, and analyzed by one-way ANONA with Dunnett's multiple comparisons test. Scale bars, 10 μm.

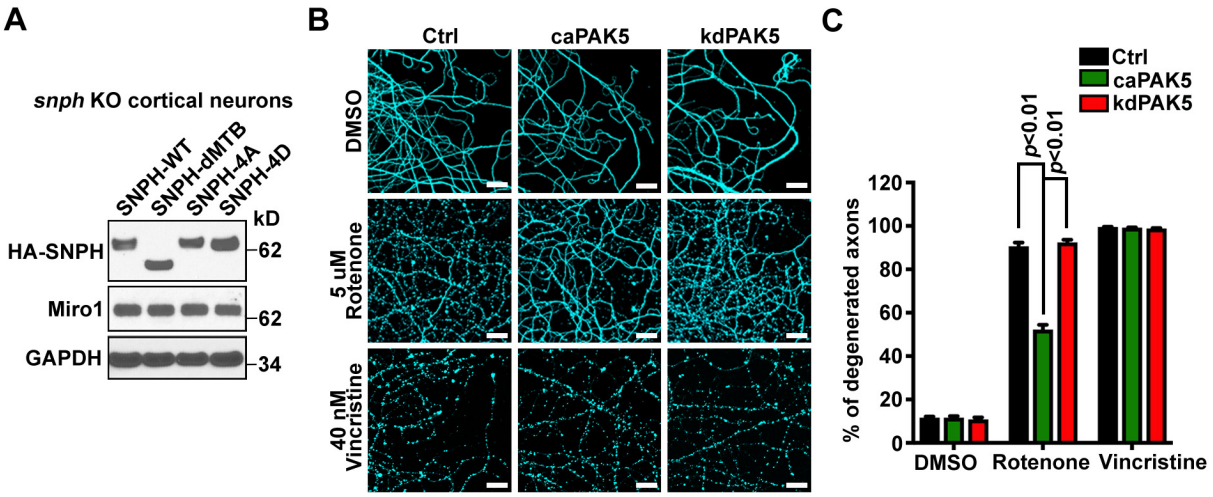

Figure S5. **Activating PAK5 protects axons from degeneration upon mitochondrial stress. Related to Figure 6**

(A) Expression of lentivirus-encoded HA-tagged SNPH or its mutants in *snph* KO cortical neurons. Neurons were infected with lentiviruses at DIV7, and cell lysates were collected at DIV14, loaded (8 μg), and sequentially immunoblotted with antibodies as indicated.

(B and C) Images (B) and analysis (C) showing that activating PAK5 reduces axon degeneration in response to mitochondrial stress. Cortical neurons in microfluidic devices were infected with lentiviruses encoding HA-tag, HA-tagged caPAK5, or kdPAK5 at DIV8. Axon chambers at DIV14 were loaded with DMSO, 5 μM Rotenone, or 40 nM Vincristine for 24 hours, followed by immunostaining with βIII-tubulin. The percentage of degenerated axons showing bead-like structures or fragmentation was quantified.

Data were quantified from n = 30 axonal images in > 3 microfluidic devices per condition from three independent experiments, expressed as mean ± SEM, and analyzed by one-way ANOVA with Dunnett's multiple comparisons test. Scale bars, 25 μm.

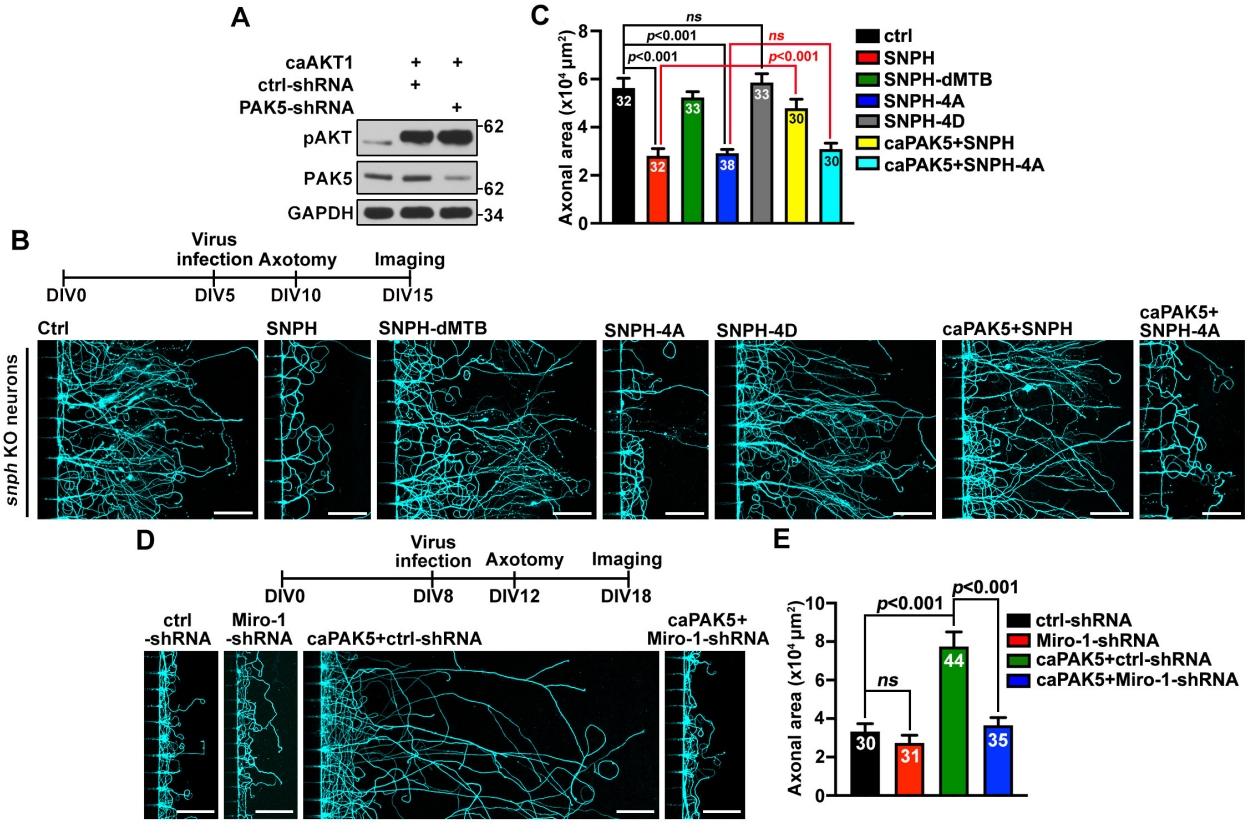

Figure S6. Reprogramming the AKT-PAK5-SNPH axis boosts CNS neuron regeneration. Related to Figure 7

(A) Immunoblots showing the expression of constitutively active AKT1 (caAKT1) in cortical neurons. Neurons at DIV7 were infected with lentiviruses encoding HA-tag control or HA-caAKT1 with control shRNA or PAK5-shRNA. Cell lysates were collected at DIV14, and equal amounts (8 μg) were loaded and sequentially immunoblotted with the indicated antibodies.

(B and C) Images (B) and analysis (C) showing regenerative capacity in *snph* KO cortical neurons after expressing phospho-dead SNPH-4A or phospho-mimicking SNPH-4D. A schematic diagram showing the timeline of virus infection, axotomy, and imaging (upper, B). Note that re-introducing SNPH or SNPH-4A, but not SNPH-4D, into *snph* KO neurons inhibits regeneration, while caPAK5 rescues regeneration upon co-expression with SNPH in *snph* KO neurons.

(D and E) Images (D) and analysis (E) showing that PAK5-enhanced regeneration requires mitochondrial transport after axotomy. A schematic diagram showing the timeline of virus infection, axotomy, and imaging (upper, D). Cortical neurons in microfluidic devices were infected with lentiviruses encoding ctrl-shRNA, Miro-1-shRNA, caPAK5 and ctrl-shRNA, or Miro-1-shRNA at DIV8, followed by axotomy at DIV12 and imaging at DIV18. Axons were labeled with βIII-tubulin. The normalized area of regenerated axons was calculated and normalized to the control. Note that inhibiting mitochondrial transport by depleting Miro-1 abolishes PAK5-enhanced regeneration.

Data were quantified from *n* = 30-44 images as indicated within bars in > 3 microfluidic devices per condition from three independent experiments, expressed as mean ± SEM, and analyzed by one-way ANOVA with Tukey's multiple-comparisons test. Scale bars, 100 μm.

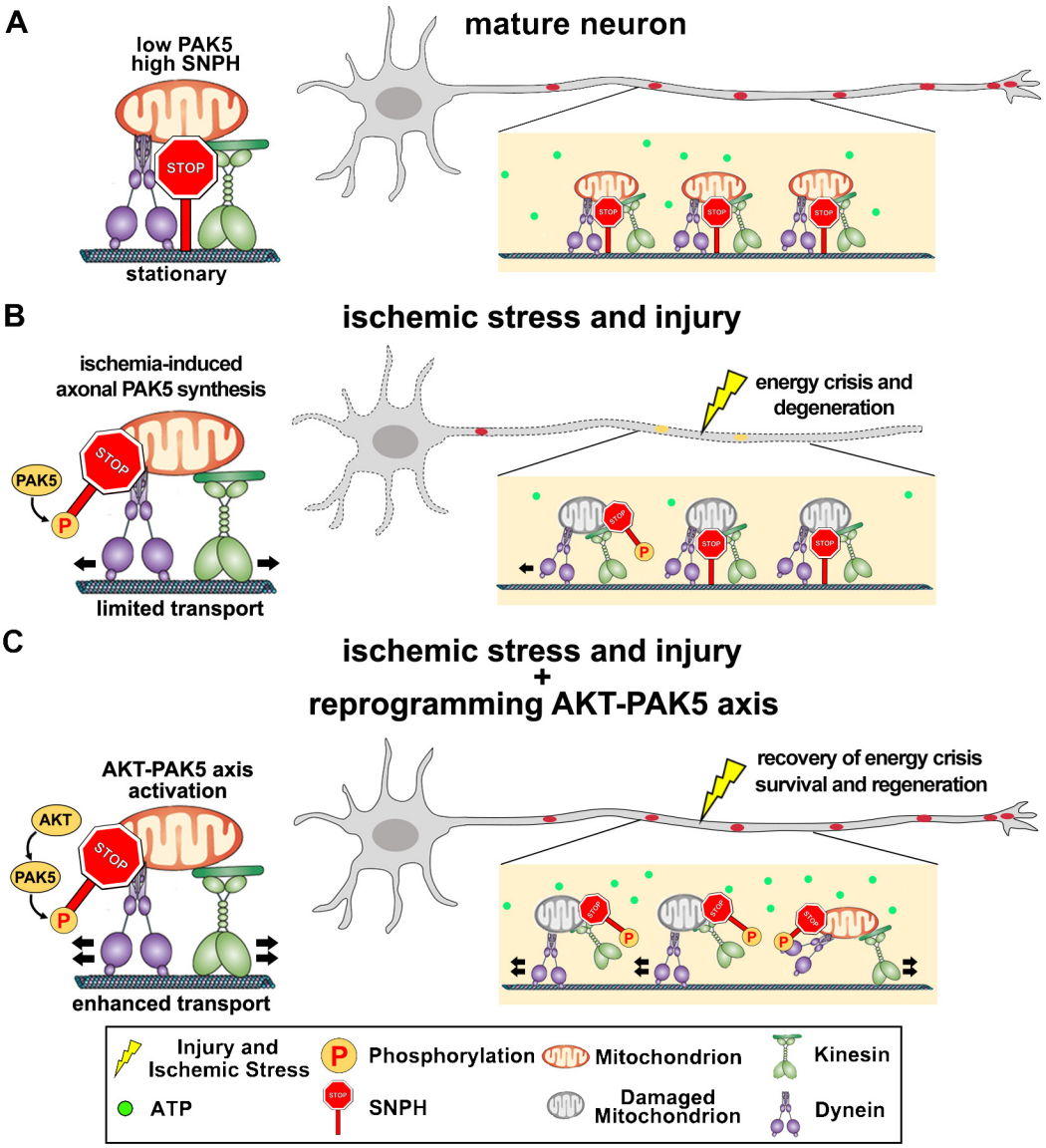

Figure S7. Reprogramming the AKT-PAK5 axis protects against axonal energy crisis and supports regeneration after acute injury-ischemia. Related to Figure 1

Mitochondria are the main cellular powerhouses that provide most of the ATP required in the brain, where a constant ATP supply is essential for neuron growth, function, survival, and regeneration. Given their unique morphological features, neurons face exceptional challenges to maintain energy homeostasis in distal axons and growth cones. The majority of axonal mitochondria remain stationary in distal axons and synapses in mature neurons and adult nervous systems due to increased expression of axonal mitochondrial anchoring protein SNPH and reduced expression of PAK5 (A). Although anchored mitochondria ideally serve as local energy sources, they need to be removed and replaced when aged or damaged. Axon injury or ischemic stress triggers acute mitochondrial damage leading to local energy crisis. The increased expression of SNPH and declined mitochondrial transport with neuron maturation contribute to CNS regeneration failure (B). Thus, enhancing mitochondrial transport by turning off SNPH-anchoring switch helps to remove damaged mitochondria and deliver healthy ones into injured axons, thus recovering energy supply and meeting increased energy requirements during repair

and regeneration. The AKT-PAK5-SNPH axis represents an intrinsic “energy repair program” that acts as the first line of axonal energy surveillance in response to injury-ischemic insults. Reprogramming an enhanced AKT-PAK5-SNPH signaling in mature neurons plays a critical role in maintaining axonal energy supply, protecting axon survival, and thus promoting regeneration after brain injury and ischemia (C).